Deterministic mapping of reservoir heterogeneity in Athabasca oil sands using surface seismic data

YONG XU and SATINDER CHOPRA, Arcis Corporation, Calgary, Canada

Bitumen reserves in oil sands in Alberta, Canada, represent one of the biggest such deposits in the world. The Athabasca region contains the bulk of this resource and the lower Cretaceous McMurray Formation contains the most significant target interval. Inclined heterolithic strata and associated sand accumulations comprise most of the formation. However, the distribution of bitumen in the formation varies due to the high degree of facies heterogeneity throughout the deposit. This lithological heterogeneity causes difficulties in interpreting geology and estimating the bitumen distribution.

Surface seismic data could play an important role in characterizing the subsurface heterogeneity because they provide lateral and vertical coverage and a link to rock physics through AVO. However, most (with notable recent exceptions using deterministic LMR shown by Bellman, 2007, and Evans and Hua, 2008) applications of surface seismic in Athabasca have been to provide attributes for statistical and neural-network predictions (Tonn, 2002; Anderson et al., 2005). The relationships between seismic data and lithology are determined at the well-control points by multivariate analysis or neural networks and then the lithology between wells is predicted from these relationships. However, interpreters often find these relationships less straightforward than conventional techniques.

In this article, we describe a two-step approach to understand the heterogeneity of Athabasca oil-sand reservoirs. The first step involves a rock physics study to understand the relationship between lithology and the related rock parameters, and pick lithology-sensitive rock parameters that can be seismically derived. The second step is deriving the chosen parameters from the seismic data.

We demonstrate this method with a case history that begins with rock physics analysis of an Athabasca reservoir zone using well-log data, and then uses seismic inversion to derive the lithology-sensitive parameters from a 2D profile. For the case study presented here, the derived results are encouraging as they calibrate with the available log curves and a blind well test confirmed the accuracy of the calibration.

Rock physics analysis

We begin the rock physics analysis by crossplotting (Figure 1) different pairs of parameters for the McMurray Formation reservoir which is at a depth of about 100 m. Figure 1a shows a strong linear correlation between bulk density and gamma ray. Clean sand samples have average densities of 2.075 g/cc with average gamma-ray values of API 25, whereas 100% shale has an average density of 2.24 g/cc with average gamma-ray value of API 85. If a linear relationship between gamma ray and shale volume (Vshale) is assumed, then Vshale can be estimated from density by using the relation Vshale = (density - 2.075)/0.165. Figure 1b reveals a weak correlation between gamma ray (shale volume) and V_P/V_S. Since P impedance can be accurately derived from seismic data, it is always desirable to look for any strong correlation between impedance and another rock parameter of interest. However, as seen in Figures 1c and 1d, P impedance is unable to indicate lithology variation, since in this case, shale and sandstone have similar P-wave impedance values as shown by the uncorrelated gamma ray and density scatter.

In the Athabasca region, the depth of the McMurray Formation varies laterally from very shallow to over 600 m. Such a large variation in depth means the rock parameters in different areas exhibit different behavior due to varying overburden compaction. Figure 2 shows crossplots from a McMurray reservoir at a depth of 400 m in an area different from the one under study. These crossplots suggest good correlation between P-impedance and density. Consequently, the relationship between these parameters could be a lithology indicator, though density as such is still a good indicator. Thus, rock physics analysis in a given area is important for, first, determination of those rock parameters that may exhibit some useful lithology-correlated relationship and, then, using this relationship to estimate such attributes from seismic data.

Workflow for mapping reservoir heterogeneity

Figure 3 shows our workflow for mapping reservoir heterogeneity in the study area. This workflow is based mainly on conventional P-wave surface seismic, though we believe it can be extended to incorporate multicomponent data. As stated earlier, due to the heterogeneity within the formation and weak correlation between seismic (P impedance or reflectivity) and lithology, "normal" attempts at geologic interpretation usually prove futile. We address this problem by using AVO attributes from surface data.

Since the reservoir is shallow and seismic data usually have sufficiently high resolution in shallow zones, it was expected that reasonably convincing estimates of reservoir heterogeneity could be obtained. Note that our approach should not in any way discourage the application of statistical methods for the same goal. When more than a couple of seismic attributes are available, neural-network approaches could determine reservoir properties within the interval of interest. However, we emphasize that the approach in this work for estimating the lithology-sensitive density reflectivity attribute provides good quality control and validation with well ties.

Improved three-term AVO inversion

Linearized three-term AVO inversion is commonly used to extract P-, S- and density reflectivity from prestack seismic data. But straightforward application on a sample-by-sample basis can generate unreliable solutions. This is due to the

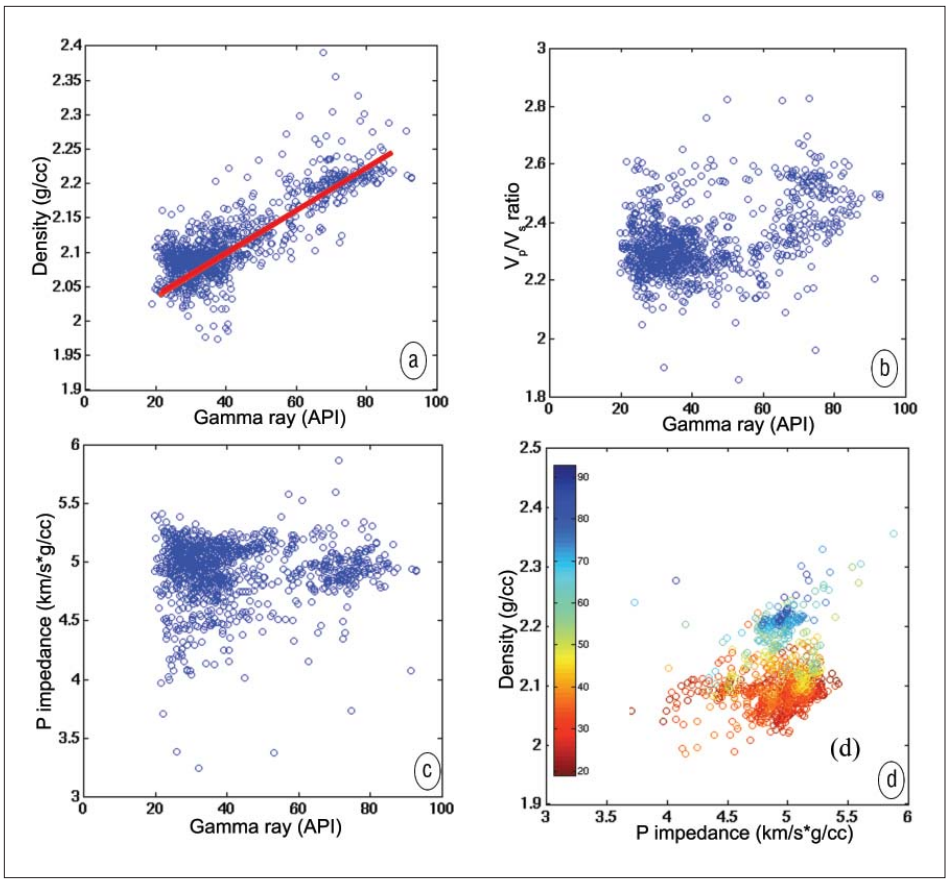

Figure 1. *Crossplots of (a) density versus gamma ray, (b) V_p/V_s versus gamma ray, (c) P impedance versus gamma ray, and (d) density versus P impedance, with colors coded by gamma-ray values. Data samples come from McMurray Formation in four wells in the Athabasca oil sands. Reservoir depth is 100 m. A linear relationship between density and gamma ray (red line in Figure 1a) can be used to estimate Vshale (or pseudo-gamma ray) from density.*

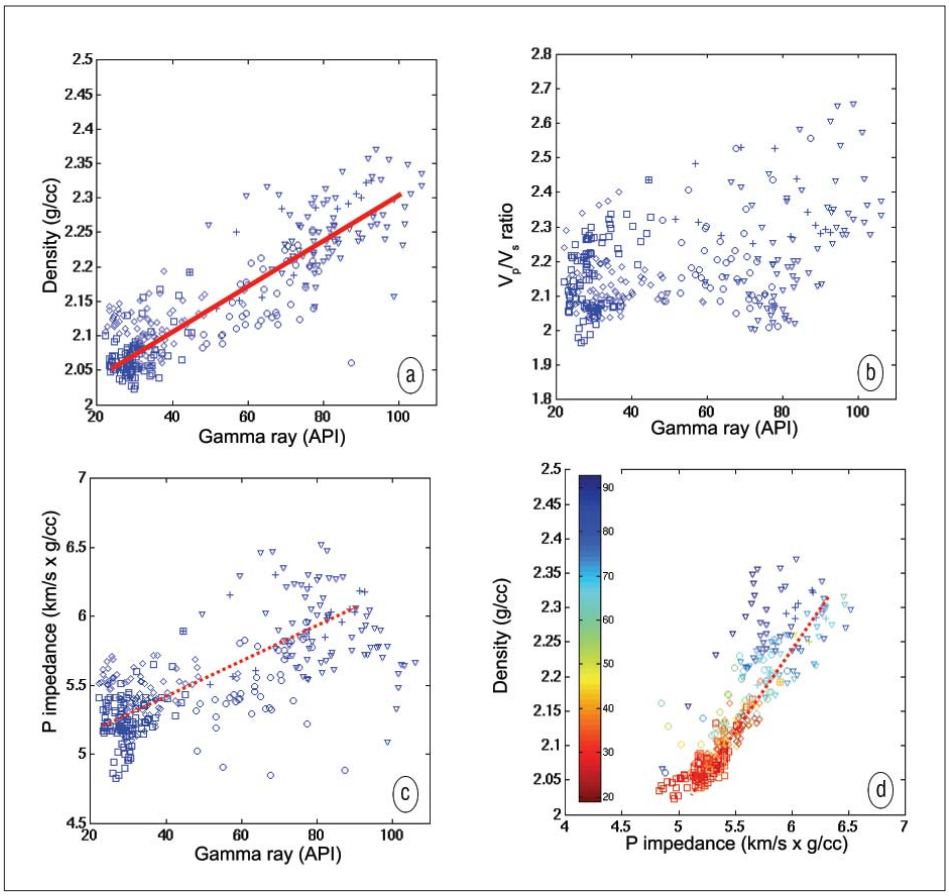

Figure 2. *Crossplots of rock physics parameters using samples from an Athabasca oil-sands well in a different area than the study area. Crossplots are arranged in the same way as in Figure 1. The McMurray reservoir is at a depth of about 400 m. While the correlation between density and gamma ray is strong, the correlation between P-impedance and gamma ray is much stronger compared with Figure 1. This can be seen in (c) and (d).*

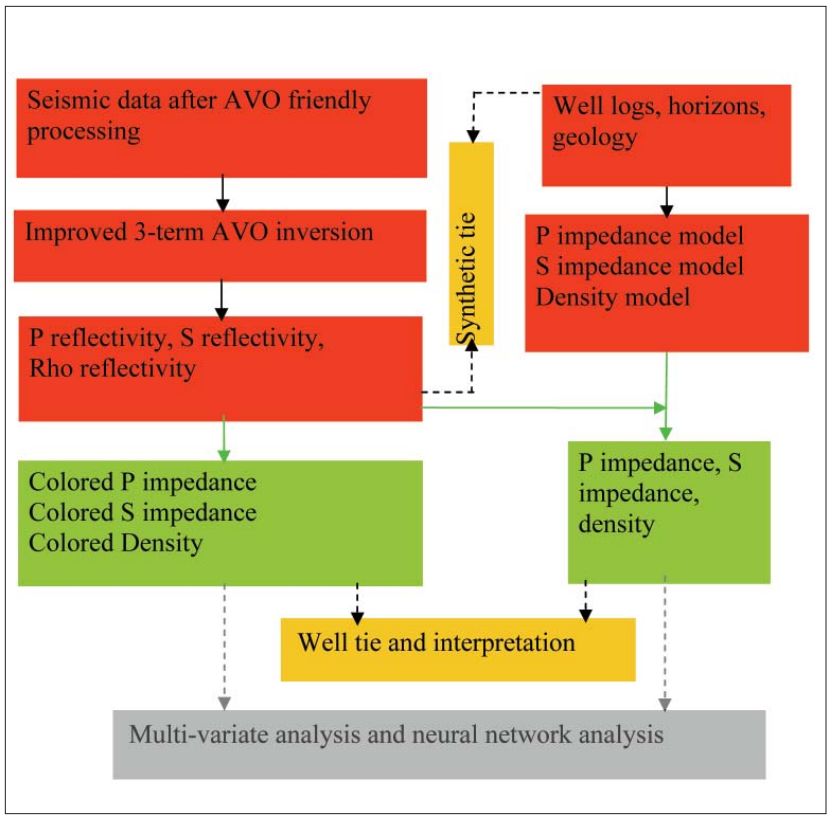

Figure 3. *Workflow of deterministic interpretation of reservoir heterogeneity of oil sands using seismic data. This approach combines rock physics with a reliable inversion, and quality control including synthetic and well-tie calibration with colored seismic attributes.*

ill-posed nature of the inverse problem, necessitating the use of certain constraints for stabilizing the inversion. Furthermore, large incident angles are required for reliable results from three-term inversion (Downton and Lines, 2001; Roy et al., 2006). Besides this, the use of statistical constraints in the inversion yields a solution that usually exhibits a reasonable variance but underestimates the lithology anomalies of interest.

Our method improves the three-term linear AVO inversion by (1) using a windowed approach instead of a sample-by-sample basis; (2) applying error-based weights in the frequency domain; (3) reducing the uncertainty of the inverse problem; (4) accounting for the strong reflection from the McMurray-Devonian interface; and (5) reducing the distortion due to NMO stretch and the related offset-dependent tuning. This results in a more reliable inversion process and also relaxes the requirement for large angles in the inversion.

Figure 4 compares the density reflectivity derived by the application of different AVO inversion methods on a synthetic gather that has an angle range of 0–40°. The true density reflectivity used to evaluate the inversion is calculated using the density log. The results clearly demonstrate that the density reflectiv-

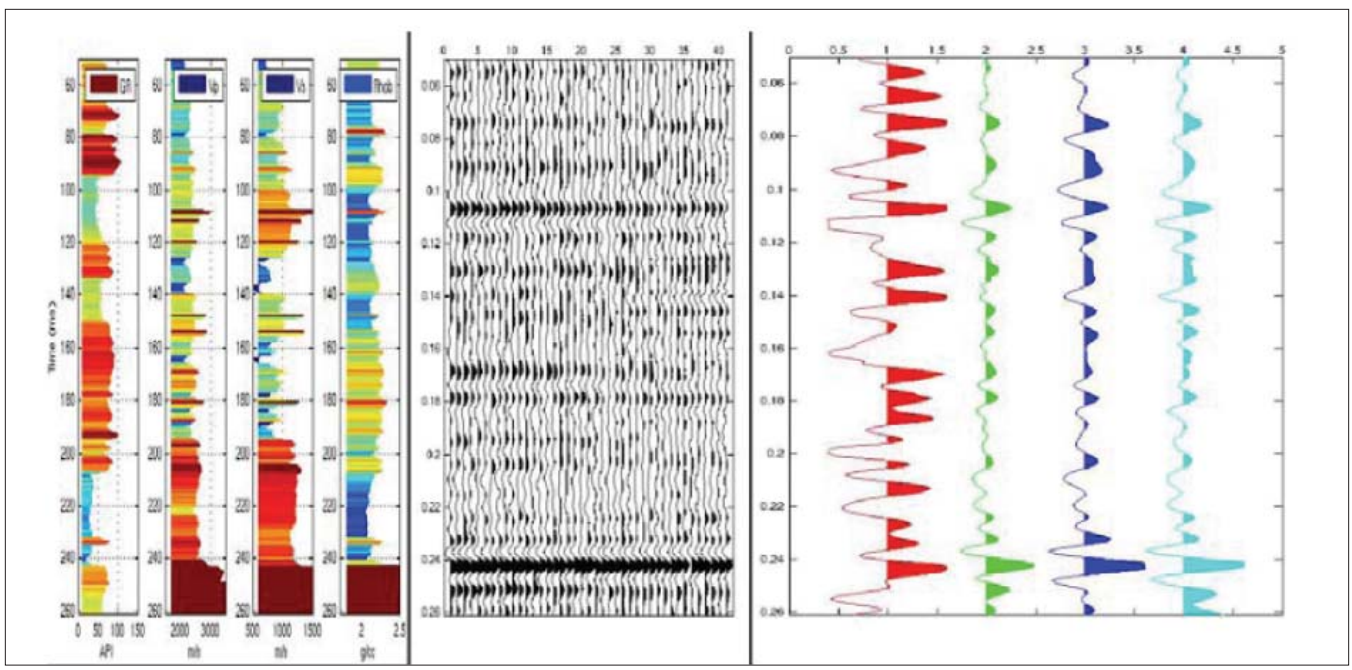

Figure 4. *Comparison of density reflectivity derived by application of different AVO inversion methods on a synthetic gather. Well logs to generate synthetic gather are shown on the left panel. The synthetic gather in the middle panel (inclusive of noise) is sorted with respect to angle and the range of angles used is from 0° (left) to 40° (right). On the right panel, the red trace is density reflectivity obtained from the application of least-squares inversion and scaled down three times for display; the green trace is obtained after application of Bayesian-constrained AVO inversion; the blue trace is the true density reflectivity calculated from the density log and the cyan trace on the extreme right is obtained by the application of the improved three-term AVO inversion. Clearly, the three-term AVO estimate shown in the cyan trace is very close to the true density reflectivity and is also superior to reflectivities derived by other methods.*

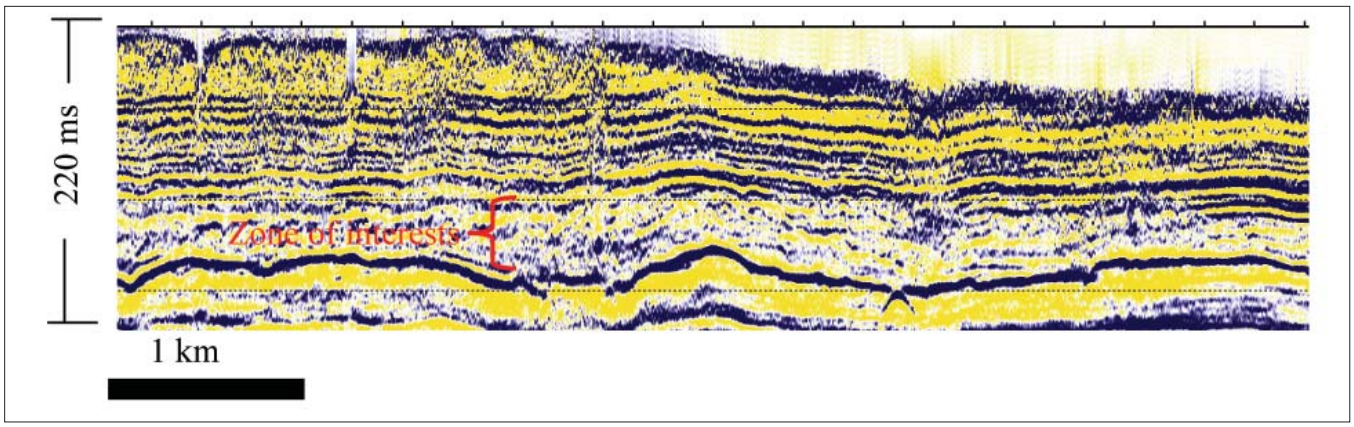

Figure 5. *Stack section showing the zone of interest.*

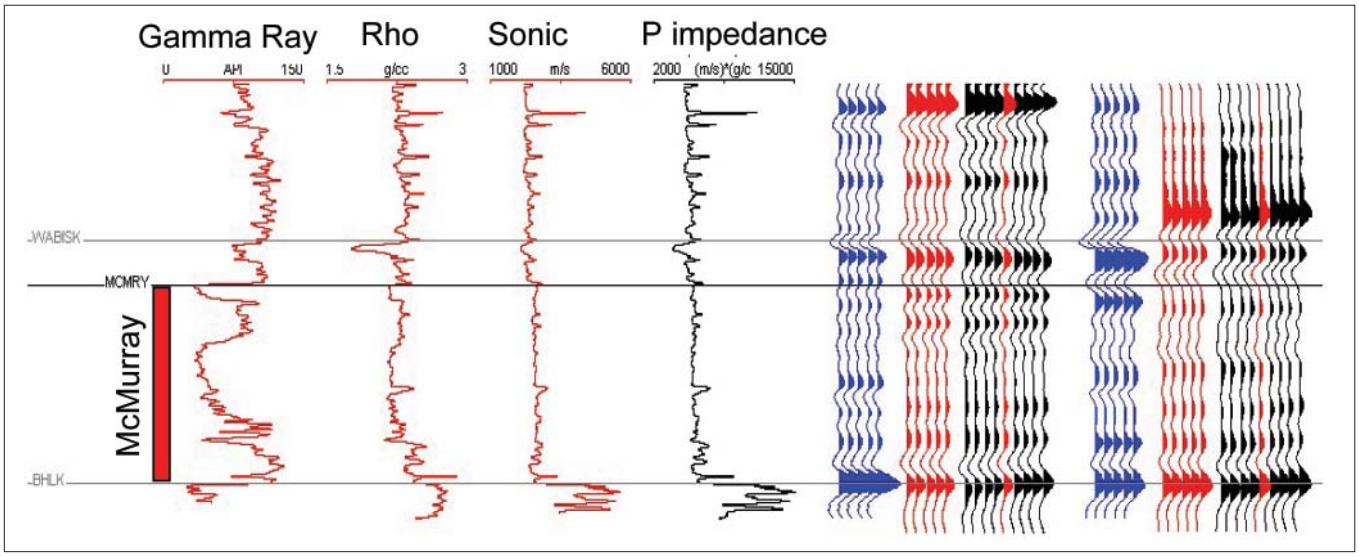

Figure 6. *Synthetic tie with AVO derived reflectivities. Blue traces are synthetic reflectivity; red traces are inverted reflectivity at well location; black traces are portion of inverted reflectivity section at well location. Left group of traces are P reflectivity, and right group of traces are density reflectivity.*

ity derived by the improved three-term inversion is closer to the true reflectivity than the density reflectivities derived by other methods.

Application to real data

A 2D seismic profile running through 11 wells in the study area was taken through an amplitude-preserved AVO processing flow. Data quality was reasonably good, and the usual noise problems in terms of ground roll and other wave modes were skillfully tackled using adaptive and iterative noise-attenuation schemes. The surface elevation variation along the profile is about 45 m, and this is of the same order as the reservoir depth variation of 55–90 m. This elevation variation was a significant factor regarding the amplitude recovery and the stability of the AVO inversion at the reservoir level. Care was exercised for amplitude recovery and superbinning was part of the data conditioning for AVO inversion. Figure 5 shows a stacked section for the seismic profile with the zone of interest indicated.

Figure 6 shows log curves and synthetics for a typical well and their correlation with the derived P impedance and density reflectivities from seismic data. The correlation between the two pairs of reflectivities is reasonably good and encouraging. Figure 7 shows the results of different AVO attributes derived as per the workflow in Figure 3. The density reflectivity derived after AVO inversion is shown in Figure 7a.

Colored density was derived from density reflectivity after simple trace integration without using density logs from wells, and this result (Figure 7b) indicates the richest sand areas (dark green) are in the middle of the McMurray Formation with a good seal cap in the upper McMurray around wells 5 and 6. These are verified by the overlain gamma-ray log curves.

Next, the density logs from all the wells except wells 3 and 7 (not available at the time) were used to generate a density model. Model-based poststack inversion was performed on density reflectivity utilizing the density model to generate a density section (Figure 7c). This section has higher resolution than the colored density and better matches the log curves. The linear relationship indicated on the crossplot between density and gamma ray (Figure 1a) was used to transform the derived density section into a Vshale section (Figure 7d). Two

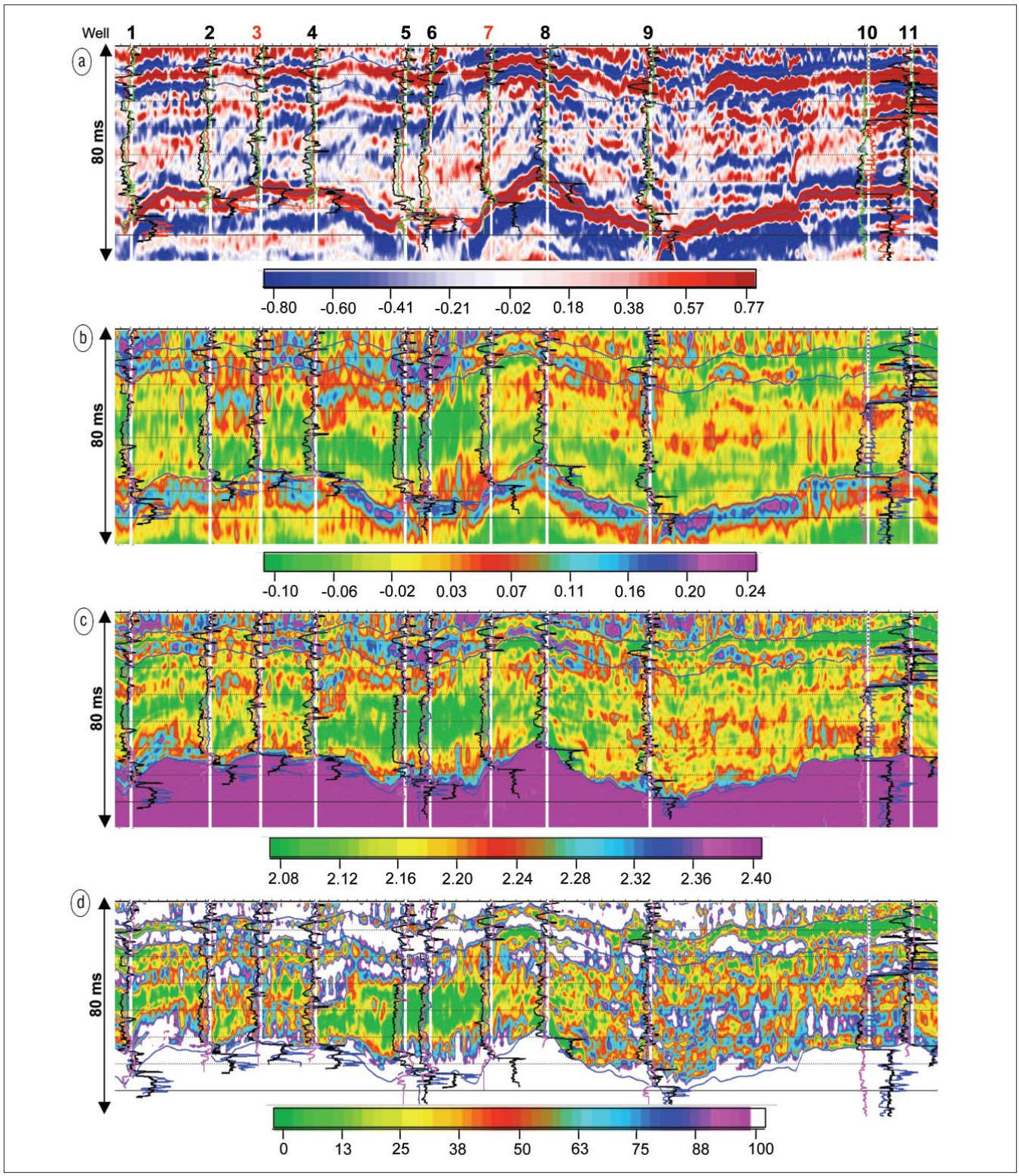

Figure 7. *Top panel (a) is the density reflectivity; second panel (b) is the colored density—the trace-integration version of density reflectivity; third panel (c) is the density section from model based inversion; bottom panel (d) is V-shale transformed from density in the third panel using the linear relationship between density and gamma ray shown in Figure 1a. Log curves are overlaid on the section. In panels (b), (c), and (d), the black curves are density logs, the purple are gamma ray logs, and the blue are impedance logs. No density logs are used in the derivation of (b), and density logs from all wells except well 3 and well 7 and horizons are used to generate a density model to derive (c) from (a) using model-based post-stack inversion. The middle McMurray is usually the reservoir while the upper McMurray is cap rock. The richest sand areas (dark green) within mid-McMurray are around wells 5 and 6 with good shaley cap rocks in upper McMurray, and these are verified by gamma-ray logs of both wells. Recently drilled well 3 and well 7 are served as blind well tests. well 3 is mainly shaley within McMurray and the density inversion result verifies this. well 7 is drilled at the edge of the richest sand zone and its reservoir also matches the inversion results. In addition, the sandy cap rock within upper McMurray in well 7 is convincingly predicted by the inversion.*

recently drilled wells (3 and 7) were used in a blind test; well 3 is mainly shaley within the McMurray and the density inversion result verifies this. Well 7 indicates good sand in the middle McMurray, but a sandy cap in the upper McMurray. These results are clearly confirmed on the inverted density (Figure 7c) and the derived Vshale sections (Figure 7d). The same results are seen on the colored density sections.

All four derived density estimate sections in Figure 7 yield encouraging confirmation with well logs and exhibit believable lateral variation in reservoir heterogeneity within the target zone.

Conclusions

A new workflow using rock physics analysis and an improved three-term AVO inversion to map reservoir heterogeneity has been demonstrated on a case study from the Athabasca oil sands in Alberta. Rock physics analysis helps find a relationship between lithology and seismically-driven elastic attributes and pick out lithology-sensitive parameter(s). In the present study, density is closely correlated with lithology. However, with increasing depth of burial, other rock physics parameters such as acoustic impedance may also correlate with lithology. The density reflectivity is reliably derived from 2D data in the area using the improved three-term AVO inversion. Other attributes derived from density reflectivity, confirmed with calibration to existing well-log data, have further provided convincing calibration to the two recently drilled wells.

The discussed workflow has successfully demonstrated a methodology for mapping heterogeneity in oil-sand reservoirs. Considering the importance of the characterization of oil-sand reservoirs in Alberta and other places around the world, this methodology could have very promising applications.

Suggested reading. "A proposed workflow for reservoir characterization using multicomponent seismic data" by Anderson et al. (SEG 2005 *Expanded Abstracts*). "Oil sands reservoir characterization: a case study at Nexen/Opti Long Lake" by Bellman (CSEG 2007 *Expanded Abstracts*). "Constrained three-parameter AVO inversion and uncertainty analysis" by Downton and Lines (SEG 2001 *Expanded Abstracts*). "Early project seismic application at the Ellis River heavy oil project-maximizing the value of VSP and well data" by Enams and Hua (CSEG 2008 *Expanded Abstracts*). "Wide-angle inversion for density: tests for heavy-oil reservoir characterization" by Roy et al. (SEG 2005 *Expanded Abstracts*). "Neural network seismic reservoir characterization in a heavy oil reservoir" by Tonn (*TLE,* 2002). TLE

Acknowledgments: We thank an anonymous company for allowing us to show the data example in this case study. We thank Arcis Corporation for encouraging the development of this work and for permission to present these results.

Corresponding author: yxu@arcis.com